for the fundamental and higher order modes in microstrip," *IEEE Trans. Microwave Theory Tech.*, vol. MTT-24, pp. 456–460, July 1976.
[13] J. B. Knorr and A. Tufekcioglu, "Spectral-domain calculation of microstrip characteristic impedance," *IEEE Trans. Microwave Theory Tech.*, vol. MTT-23, pp. 725–728, Sept. 1975.
[14] R. H. Jansen, "Fast accurate hybrid mode computation of nonsymmetrical coupled microstrip characteristics," presented at 7th European Microwave Conference, Feb. 1977.
[15] R. F. Harrington, *Field Computation by Moment Methods*. New York: Macmillan, 1968, secs. 1-8, 1-7, 7-6, 1-3.
[16] I. N. Sneddon, *The Use of Integral Transforms*. New Delhi, India: Tata McGraw-Hill, 1974, pp. 42–46.
[17] R. Mittra and S. W. Lee, *Analytical Techniques in the Theory of Guided Waves*. New York: Macmillan, 1971, pp. 4–11.
[18] P. Silvester and P. Benedek, "Electrostatics of the microstrip-revisited," *IEEE Trans. Microwave Theory Tech.*, vol. MTT-20, pp. 756–758, Nov. 1972.
[19] J. R. Westlake, *A Handbook of Numerical Matrix Inversion and Solution of Linear Equations*. New York: Wiley, 1968, pp. 88–91.
[20] E. J. Denlinger, "A frequency dependent solution for microstrip transmission lines," *IEEE Trans. Microwave Theory Tech.*, vol. MTT-19, pp. 30–39, Jan. 1971.
[21] G. Kowalski and R. Pregla, "Dispersion characteristics of shielded microstrip with finite thickness," *Electronics and Communications (AEÜ)*, vol. 25, pp. 193–196, Apr. 1971.
[22] E. O. Hammerstad and F. Bekkadal, "Microstrip handbook," ELAB Rep. STF 44 A 74169, Univ. Trondheim, Norway, Feb. 1975.
[23] G. Kompa, "The frequency dependent transmission properties of microstrip impedance steps, filters and stubs" (in German), Ph.D. dissertation, Aachen Tech. Univ., Germany, May 1975.
[24] B. Rama Rao, "Effect of loss and frequency dispersion on the performance of microstrip directional couplers and coupled line filters," *IEEE Trans. Microwave Theory Tech.*, vol. MTT-22, pp. 747–750, July 1974.
[25] S. Ramo and J. R. Whinnery, *Fields and Waves in Modern Radio*. New York: Wiley, 1953.
[26] R. Horton, "Loss calculations of coupled microstrip lines," *IEEE Trans. Microwave Theory Tech.*, vol. MTT-21, pp. 359–360, May 1973.

A Simple Method for Determining the Green's Function for a Large Class of MIC Lines Having Multilayered Dielectric Structures

RAYMOND CRAMPAGNE, MAJID AHMADPANAH, AND JEAN-LOUIS GUIRAUD

Abstract—**To find the characteristic parameters of the wave propagation in microstrip structures, several Green's function methods have already been developed, corresponding to particular geometric configurations. In this paper, three of these methods are synthesized, showing that the final equations in the different cases are identical. Moreover, using the transverse transmission line theory, the Green's function is solved numerically for an *N*-layer dielectric structure.**

I. Introduction

MICROSTRIP transmission lines are largely used in the microwave integrated circuits. Although being a simplifying approximation, the quasi-TEM approximation is well known to have proved useful in giving quite accurate results for practical purposes. The characteristic parameters of such lines have been calculated, using various methods. The method utilizing Green's potential function lets one transform a differential equation to an integral one; where the unknown quantity becomes the charge density. This is solved easily by numerical techniques using the moment and the point matching methods.

In this method, the conductor geometry can be defined exactly; in particular the conductor's thickness and the dissymetry in the strip configuration can be taken into account. However, we assume infinitely thin symmetric conductors because these parameters do not modify the determination of the Green's function.

The present paper tries to generalize the studies done on microstrip lines with two or three layers of dielectric [1]–[3] in that it determines the Green's function for multilayer microstrip lines having the same conductor geometry as used in previous studies. Our main aim had been at presenting the results in analytic form which lends itself to numeric solution, requiring very little modification in the programs already existing.

Manuscript received January 13, 1977; revised April 5, 1977.

R. Crampagne and M. Ahmadpanah are with Laboratoire de Microondes, 2, rue Camichel—31 071 Toulouse, France.
J. L. Guiraud is with Laboratoire de Physique Mathématique, 118, route de Narbonne—31 077 Toulouse, France.

0018-9480/78/0200-0082$00.75

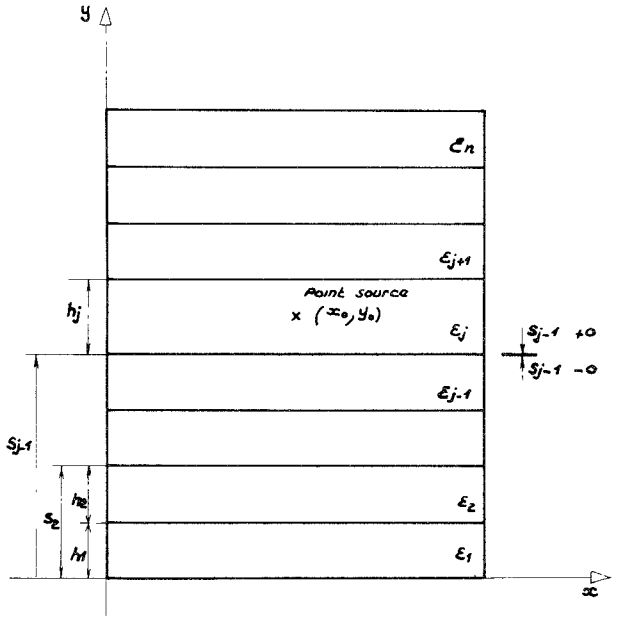

Fig. 1. The geometric configuration for determining the Green's function in a rectangular region; definition of notations.

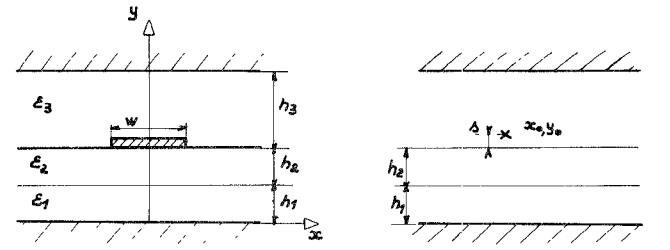

Fig. 2. (a) The triplate configuration. (b) The corresponding geometry for determining the Green's function ($s \to 0$).

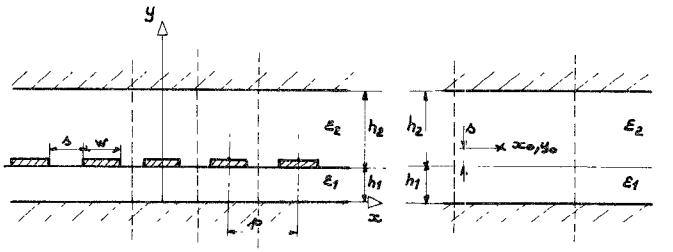

(a) (b)

Fig. 3. (a) Array of periodic conductors. (b) The elementary cell for determining the Green's function ($s \to 0$).

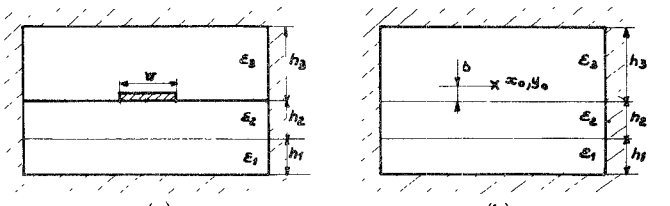

(a) (b)

Fig. 4. (a) Microstrip with rectangular sidewalls. (b) The corresponding geometry to calculate the Green's function ($s \to 0$).

II. Use of the Green's Function

For a unit charge located at (x_0,y_0), the Green's function should satisfy, by definition, the Poisson's differential equation in the plane (x,y):

$$\nabla_t^2 G(x,y\,|\,x_0,y_0) = \frac{1}{\varepsilon}\delta(x-x_0)\cdot\delta(y-y_0) \tag{1}$$

using the notations of Fig. 1, the following boundary conditions should be applied to each dielectric interface:

$$G(x, s_j - 0) = G(x, s_j + 0) \tag{2a}$$

$$\varepsilon_j \frac{\partial}{\partial y}[G(x, s_j - 0)] = \varepsilon_{j+1}\frac{\partial}{\partial y}[G(x, s_j + 0)]. \tag{2b}$$

Figs. 2(a), 3(a), and 4(a) illustrate the configurations used in practice, while Figs. 2(b), 3(b), and 4(b) show the corresponding geometries which permit the determination of the Green's function. Depending on the type of the configuration, several methods have been used to transform the differential equation (1) with two variables, to a single variable differential equation, integrable analytically.

To solve the problem of an inhomogeneous triplate, Figs. 2(a) and (b), Yamashita, [1] expands the Green's function in a Fourier transform in the x-coordinate:

$$\tilde{f}(\beta) = \int_{-\infty}^{+\infty} f(x)e^{j\beta x}\,dx.$$

So, equation (1) is expressed as the following differential equation:

$$\left(\frac{d^2}{dy^2} - \beta^2\right)\tilde{G}(\beta,y) = -\frac{1}{\varepsilon}\tilde{\rho}(\beta)\cdot\delta(y-y_0) \tag{3}$$

where $\tilde{G}$ and $\tilde{\rho}$ are the Fourier transforms of the Green's function and the unit charge, respectively. The boundary conditions, satisfied by $\tilde{G}$ lead to the equations similar to (2a) and (2b).

In the second configuration, Fig. 3(a) and (b), with which the microstrip periodic structures can be analyzed, Weiss [3] expands the solution in the form of space harmonics, using the fact that the medium is invariant by a translation p along the x-coordinate,

$$G(y,x\,|\,y_0,x_0) = \sum_{m=-\infty}^{+\infty} G_m(y)e^{j\beta_m x}.$$

After some mathematical manipulations, equation (1) and the relation above can be written as:

$$\frac{d^2G_m}{dy^2} - \beta_m^2 G_m = -\frac{1}{\varepsilon p}\exp(-j\beta_m x)\cdot\delta(y-y_0). \tag{4}$$

Here again, the continuity conditions satisfied by are similar to those in (2).

Figs. 4(a) and (b) illustrate the configurations which correspond to the microstrip line with rectangular side walls, [4].

This is only a particular case of a problem which can give rise to eight different cases, depending on whether the

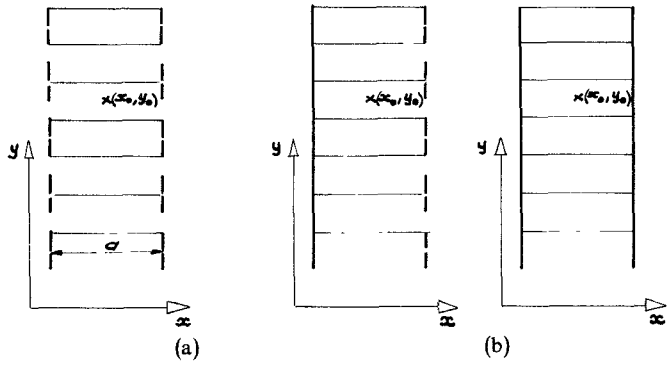

Fig. 5. Classification based on the boundary conditions. The thick solid lines represent the electric walls, the dashed lines correspond to the magnetic walls and the dielectric interfaces are specified by the thin solid lines.

rectangular walls satisfy the boundary conditions of Dirichlet type (electric wall, $G = 0$), or of Neumann type (magnetic wall, $\partial G/\partial n = 0$).

We shall show that using the transverse transmission line method, the boundary conditions on the lower and the upper surfaces can be taken into account. Hence the eight cases mentioned above can be reduced to three, as shown in Fig. 5, where the conditions on the horizontal walls can be arbitrary.

As in [2], the Green's function can be expressed as the sum of the product of elementary functions with separated variables:

$$G = \sum_{n=1}^{\infty} G_n^y(y) \cdot G_n^x(x) \tag{5}$$

in order to satisfy the boundary conditions on the vertical walls, the following expressions are found for $G_n^x(x)$, for the three cases of Fig. 5:

$$\text{case 4(a):} \quad G_n^x(x) = \cos \frac{n\pi x}{a}, \qquad n = 2, 3, \cdots \infty,$$

$$\text{case 4(b):} \quad G_n^x(x) = \sin (2n+1)\frac{\pi x}{2a}, \qquad n = 1, 2, \cdots \infty,$$

$$\text{case 4(c):} \quad G_n^x(x) = \sin \frac{n\pi x}{a}, \qquad n = 1, 2, \cdots \infty.$$

using these expressions in equation (5) and noting that the functions $\sin (n\pi x/a)$, $\cos (n\pi x/a)$, and $\sin (2n+1)(\pi x/2a)$ are orthogonal in the interval $(0,a)$, the following differential equations are obtained:

$$4(a) \Rightarrow \frac{d^2G_n^y}{dy^2} - \left(\frac{n\pi}{a}\right)^2 G_n^y = -\frac{2}{a\varepsilon}\delta(y - y_0) \cos \frac{n\pi x_0}{a} \tag{6}$$

$$4(b) \Rightarrow \frac{d^2G_n^y}{dy^2} - \left[(2n+1)\frac{\pi}{2a}\right]^2 G_n^y = \frac{2}{a\varepsilon}\delta(y - y_0) \sin (2n+1)\frac{\pi x_0}{2a} \tag{7}$$

$$4(c) \Rightarrow \frac{d^2G_n^y}{dy^2} - \left(\frac{n\pi}{a}\right)^2 G_n^y = -\frac{2}{a\varepsilon}\delta(y - y_0) \sin \frac{n\pi x_0}{a}. \tag{8}$$

Again, the functions G_n^y should satisfy the boundary conditions similar to (2).

The differential equations (3), (4), (6), (7), and (8) and the corresponding boundary conditions, have in general been solved for a very few number of dielectric layers, because the method, consisting of satisfying the boundary conditions on each dielectric interface, leads to a system of linear equations of $2N$ rows (N being the number of the dielectric layers). To overcome this difficulty, some authors [4] have tried to generalize the problem. We shall show that the equations in [4], which are mathematically exact, can be formulated by a much simpler method and easier to treat numerically. Moreover, we will consider some more general geometries (Figs. 2(b), 3(b), and 4(b)).

At first, we note that all of the differential equations already found (equations (3), (4), (6), (7), (8)) are identical, just as are the boundary conditions.

So, the functions $\tilde{G}(\beta)$, G_m, and G_n^y can be determined by similar methods. Moreover, the differential equation satisfied by these functions and boundary conditions, can be identified with the equations satisfied by the voltage and the current along a transmission line.

III. The Transverse Transmission Line Method

Consider a transmission line with a current source of intensity I_s at $y = y_0$. The voltage and current relations along the line are [5]–[7]:

$$\frac{dV}{dy} = -\gamma Z_c I \tag{9}$$

$$\frac{dI}{dy} = -\frac{\gamma}{Z_c} V + I_s \cdot \delta(y - y_0) \tag{10}$$

where Z_c is the characteristic impedance of the line and γ is the propagation constant. Equations (9) and (10) solved simultaneously lead to a differential equation satisfied by the voltage:

$$\frac{d^2V}{dy^2} - \gamma^2 V = -\gamma Z_c I_s \cdot \delta(y - y_0). \tag{11}$$

In the case of the change in the characteristic admittance of the line, the continuity conditions are

$$V_i = V_{i+1} \tag{12a}$$

and $I_i = I_{i+1}$ which combined with (9) give:

$$Y_{ci}\frac{\partial V_i}{\partial y} = Y_{ci+1}\frac{\partial V_{i+1}}{\partial y}. \tag{12b}$$

Comparing (11), (12a), and (12b), satisfied by the voltage along the transmission line, with those satisfied by the

TABLE I

Geometric configuration	Formula to obtain the Green's function	Differential Equation	Propagation constant	Current source
Figure 2a	$\tilde{G}(\beta)=\int_{-\infty}^{+\infty} G(x)e^{j\beta x}dx$	$\left(\frac{d^2}{dy^2}-\beta^2\right)\tilde{G}=-\frac{1}{\varepsilon}\tilde{\rho}(\beta)\delta(y-y_0)$	β	$\frac{\tilde{\rho}(\beta)}{\beta}$
Figure 3a	$G=\sum_{-\infty}^{+\infty} G_m(y)e^{j\beta_m x}$	$\left(\frac{d^2}{dy^2}-\beta_m^2\right)G_m=\frac{1}{\varepsilon_p}e^{-j\beta_m x_0}\delta(y-y_0)$	$\beta_m=\frac{\varphi+2\pi m}{p}$	$\frac{e^{j\beta_m x_0}}{\beta_m p}$
Figure 5a	$G=\sum_{1}^{\infty} G_n^y(y)\cos\frac{n\pi x}{a}$	$\left\{\frac{d^2}{dy^2}-\left(\frac{n\pi}{a}\right)^2\right\}G_n^y=-\frac{2}{a\varepsilon}\cos\frac{n\pi x_0}{a}\delta(y-y_0)$	$\frac{n\pi}{a}$	$\frac{2}{n\pi}\cos\frac{n\pi x_0}{a}$
Figure 5b	$G=\sum_{n=1}^{\infty} G_m^y(y)\sin(2n+1)\frac{\pi x}{2a}$	$\left\{\frac{d^2}{dy^2}-\left[(2n+1)\frac{\pi}{2a}\right]^2\right\}G_m^y=-\frac{2}{a\varepsilon}\delta(y-y_0)\sin(2n+1)\frac{\pi x_0}{2a}$	$(2n+1)\frac{\pi}{2a}$	$\frac{4}{(2n+1)\pi}\sin(2n+1)\frac{\pi x_0}{a}$
Figure 5c	$G=\sum_{n=1}^{\infty} G_n^y(y)\sin\frac{n\pi x}{a}$	$\left\{\frac{d^2}{dy^2}-\left(\frac{n\pi}{a}\right)^2\right\}G_m^y=-\frac{2}{a\varepsilon}\sin\frac{n\pi x_0}{a}\delta(y-y_0)$	$\frac{n\pi}{a}$	$\frac{2}{n\pi}\sin\frac{n\pi x_0}{a}$

one-dimensional Green's function, one notices the following similarities:

1) The functions characterizing the Green's function can be identified by the voltage along the line:

$$V \equiv \tilde{G}(\beta);\quad G_m(y);\quad G_n^y(y).$$

2) According to (2b) and (12b), the dielectric constant of the layer can be identified by the characteristic admittance of the transmission line.

Table I shows the identification of all of the characteristic parameters concerned in equations (3), (4), (6), (7), and (8). For example, for the configuration illustrated in Fig. 5(c), comparing (8) and (11), we obtain: $\gamma = n\pi/a$.

Taking $Y_{ci} = \varepsilon_i$ and equalizing the right-hand sides of the two equations gives the expression for the intensity of the current source:

$$I_s = \frac{2}{n\pi}\sin\frac{n\pi x_0}{a}.$$

On the same reasoning, the other values of Table I are found in a similar way. If the Green's function is to be calculated in the charge plane ($y = y_0$), according to the previous identifications, we should determine the voltage on the transmission line at $y = y_0$:

$$V = ZI_s$$

where Z is the impedance seen in the plane $y = y_0$ because of all transmission line steps of length h_i and the characteristic admittance ε_i. These steps can be terminated by short-circuits (Dirichlet's case); open circuits (Neumann's case), or by a matched charge (where the dielectric is infinitely long).

Consider the example of four dielectric layers represented in Fig. 6(a). This is a special case of the configuration

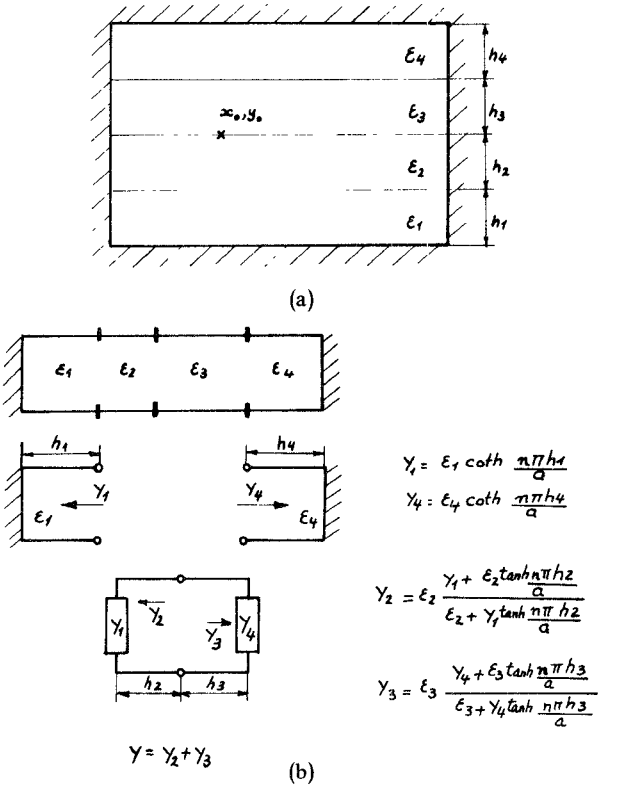

Fig. 6. (a) Microstrip with rectangular sidewalls and 4 dielectric layers. (b) Application of the transverse transmission line method.

illustrated in Fig. 5(c), where the lower and the upper walls are the short circuits. With the help of Table I, the Green's function is found to be

$$G(x,y) = \sum_n G_n^y(y)\sin\frac{n\pi x}{a},\qquad y = y_0 \tag{13}$$

where $G_n^y(y_0)$ is determined by the transverse transmission line technique Fig. 5(b). The admittance in the charge plane is

$$Y = \varepsilon_2 \cdot \frac{\varepsilon_1 \coth \frac{n\pi h_1}{a} + \varepsilon_2 \tanh \frac{n\pi h_2}{a}}{\varepsilon_2 + \varepsilon_1 \coth \frac{n\pi h_1}{a} \cdot \tanh \frac{n\pi h_2}{a}} + \varepsilon_3 \cdot \frac{\varepsilon_4 \coth \frac{n\pi h_4}{a} + \varepsilon_3 \tanh \frac{n\pi h_3}{a}}{\varepsilon_3 + \varepsilon_4 \coth \frac{n\pi h_4}{a} \cdot \tanh \frac{n\pi h_3}{a}} \quad (14)$$

referring to Table I, the source intensity is found to be equal to $2/n\pi \sin n\pi x_0/a$, and the function $G_n^y(h_1 + h_2)$ is determined by the following relation:

$$G_n^y(h_1 + h_2) = \frac{2}{n\pi} \cdot \frac{1}{Y} \sin \frac{n\pi x_0}{a}. \quad (15)$$

The resultant Green's function is found by replacing in equation (13) the values obtained in (14) and (15). Taking $h_4 = 0$, we find the formulas presented by Yamashita and Atsuki [2] in a modified form.

In this way, we are in the possession of a general theory which is independent of the number of the dielectric layers. The problem is reduced to the determination of Y, for which the following formula should be iterated:

$$Y = Y_c \cdot \frac{Y_L + Y_c \tanh \gamma l}{Y_c + Y_L \tanh \gamma l}. \quad (16)$$

For the horizontal walls, $Y_L = 0$ for Neumann and is infinity in the case of Dirichlet. In the example above, Dirichlet conditions were considered; to solve the problem with Neumann conditions, $\coth n\pi h_1/a$ and $\coth n\pi h_4/a$ must be replaced by $\tanh n\pi h_1/a$ and $\tanh n\pi h_4/a$, respectively. To find the Green's function in a plane other than that of the charge, at a distance h, the formula giving the voltage along the transmission line must be iterated:

$$V = V_L \left\{ \cosh \gamma h + \frac{Z_c}{Z_L} \sinh \gamma h \right\}. \quad (17)$$

In Fig. 6(a), for example, to find the Green's function at $y = h_1$, $G_n^y(h_1)$ is determined and using equation (17), we have

$$G_n^y(h_1 + h_2) = G_n^y(h_1) \left\{ \cosh \frac{n\pi h_2}{a} + \frac{1}{\varepsilon_2 Z_L} \sinh \frac{n\pi h_2}{a} \right\} \quad (18)$$

where Z_L is the impedance of a short-circuit at the end of a length of line h_1, that is,

$$Z_L = \frac{1}{Y_1} = \frac{1}{\varepsilon_1} \tanh \frac{n\pi h_1}{a}.$$

IV. Application

An important application of this theory is the study of the microstrip configurations whose dielectric medium has a variable dielectric constant with an index gradient in the y direction. In this case, in order to apply the method, the dielectric thickness is subdivided into N equal intervals of constant permittivity (Fig. 7). The numerical studies have shown that, for the index gradients with no abrupt variation, the characteristic parameters of the propagation tend to a limit, and that subdividing the dielectric into 30 layers is quite sufficient.

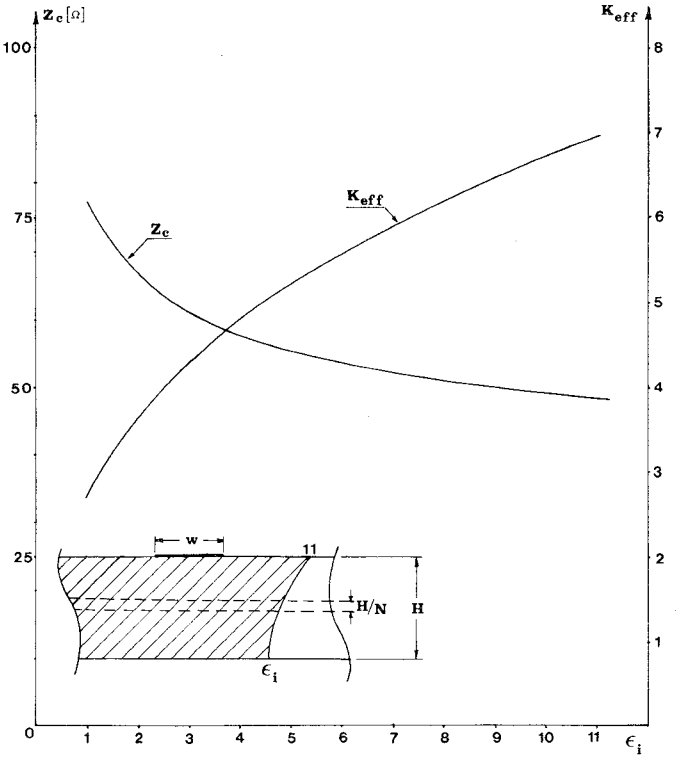

Fig. 7. Characteristic parameters of the propagation along a microstrip; the dielectric constant of the substrate having an exponential variation.

Fig. 7 illustrates the variation of the effective dielectric constant and the characteristic impedance for an exponential variation of the dielectric constant. To obtain the curves, the value of the relative permittivity has been taken constant (equal to 11) in the conductor plane, and it has been varied from 1 to 10 in the ground plane. This can be the starting point of further studies concerning the heat diffusion through a dielectric substrate, and the variation of its dielectric constant with temperature.

V. Conclusion

With the help of the transverse transmission line technique and using the equivalent expressions indicated in Table I, the case of a large number of the dielectric layers is reduced to the iteration of the formulas similar to (16) and (17). These simple formulas permit an extremely easy numerical analysis of the problem. Moreover, they permit the structures as different as a periodic array of strips and a microstrip with rectangular side walls to be analyzed identically. Using this method, the number of dielectric layers will be no more considered as an obstacle in the determination of Green's functions. Having a practical view of the

problem, one can use the computer programs already existing, with very little modification. The theory presented thus unifies all the Green's function theories used for the microstrip structures with any kind of geometry.

References

[1] E. Yamashita, "Variational method for the analysis of microstrip like transmission lines," *IEEE Trans. Microwave Theory Tech.*, vol. MTT-16, pp. 251–256, Apr. 1968.
[2] E. Yamashita and K. Atsuki, "Stripline with rectangular outer conductors and three dielectric layers," *IEEE Trans. Microwave Theory Tech.*, vol. MTT-18, pp. 238–244, May 1970.
[3] J. A. Weiss, "Dispersion and field analysis of a microstrip meander line slow-wave structure," *IEEE Trans. Microwave Theory Tech.*, vol. MTT-22, pp. 1194–1201, Dec. 1974.
[4] M. Kobayashi and R. Terakado, "General form of Green's function for multilayer microstrip line with rectangular side walls," *IEEE Trans. Microwave Theory Tech.*, vol. MTT-24, pp. 626–628, 1976.
[5] Y. Chang and I. E. Chang, "Simple method for the variational analysis of a generalized N-dielectric layer transmission line," *Electronics Letters*, vol. 6, no. 3, pp. 49–50, Feb. 5, 1970.
[6] R. E. Collin, *Field Theory of Guided Waves*. New York: McGraw-Hill, 1960.
[7] J. Vine, "Impedance networks," in *Field Analysis· Exp. and Comp. Methods*, Vitkovitch, Ed. New York: Van Nostrand, 1966.

Calculation of Electromagnetic Energy Absorption in Prolate Spheroids by the Point Matching Method

R. RUPPIN

Abstract—**The point matching method is used to calculate electromagnetic power absorption in tissue prolate spheroids irradiated by a plane wave. The calculation extends from the low-frequency region and well into the resonance region, but is restricted to spheroids of small eccentricity. A strong dependence of the absorption on the orientation and the polarization of the incident beam is found to occur, in agreement with previous experimental measurements on animals and phantom models.**

I. Introduction

IN THE THEORETICAL analysis of the interaction of electromagnetic radiation with biological bodies it is usually necessary to resort to simplified geometries. The spherical model has often been used [1]–[3] because of the availability of the Mie theory which provides an analytic solution. Recently, Gandhi [4]–[6] has determined experimentally that there exist interesting polarization effects which cannot be explained by spherical models. An important finding of his measurements was that the resonance absorption for electric polarization (electric field parallel to the long dimension of the irradiated body) was much higher than for the magnetic polarization. The prolate spheroidal model naturally arises as a candidate for the theoretical interpretation of such polarization effects. Unfortunately, this geometry is analytically tractable only in the quasi-static limit, i.e., for wavelengths much longer than the dimensions of the spheroid. A perturbative extension of the low frequency solution has been employed in the calculations of Durney *et al.* [7] and Johnson *et al.* [8]. Their results do exhibit polarization effects, but are still restricted to low frequencies (lower than 30 MHz for man-sized spheroids) and cannot give information about the important resonance region.

In this paper we employ a numerical method to calculate the absorption for higher frequencies, extending well into the resonance region, but only for spheroids with major to minor axis ratio not larger than 1.5. The point matching method used here has been reviewed by Kerker [9], and has more recently been applied to the calculation of the scattering of radio waves from raindrops [10], [11]. In the following section we briefly describe the method, using the notation of Morrison and Cross [11]. The numerical calculations are presented in Section III, and in Section IV the results are discussed and compared with previous experimental results.

II. Point Matching Method

We consider a homogeneous prolate spheroid of tissue which is irradiated by an electromagnetic plane wave of frequency ω. Let a denote the length of the semiaxis in the symmetry direction and let b denote the lengths of the other

Manuscript received December 28, 1976; revised April 20, 1977.
The author is with the Soreq Nuclear Research Centre, Yavne, Israel.

0018-9480/78/0200-0087$00.75